A Comprehensive Experimental Study on the Way the Operating Conditions of the Acid Treatment of Zeolite Affect Its Chemical, Textural, and Crystallographic Properties

Sanarya Kamal
Laboratories and Quality Control Department, North Gas Company, Ministry of Oil, Kirkuk, Iraq
sanarya.kamal1507d@coeng.uobaghdad.edu.iq

Farah Al-Jubory
Petroleum and Gas Refining Engineering Department, Petroleum Process Engineering, Tikrit University, Tikrit, Iraq
farah.k.khalaf@tu.edu.iq

Ammar Abbas
Chemical Engineering Department, College of Engineering, University of Baghdad, Baghdad, Iraq
ammarabbas@coeng.uobaghdad.edu.iq (corresponding author)

Vida Ravankhah
Chemical Engineering Department, Faculty of Engineering, Kermanshah University of Technology, Kermanshah, Iran
v.ravankhah@smail.kut.ac.ir

Received: 22 November 2025 | Revised: 14 December 2025 and 26 December 2025 | Accepted: 29 December 2025

 DOI: https://doi.org/10.48084/etasr.16443

ABSTRACT

This study used a factorial design to examine how temperature and acid treatment duration affect the properties of Na-X zeolite. Statistical analysis showed that the difference of temperature influenced the silicon-to-aluminum ratio significantly, as measured by X-ray fluorescence. On the other hand, longer treatment, significantly affected the textural and crystallographic properties as evidenced by surface area analysis and X-Ray Diffraction (XRD). Kinetic analysis revealed selective aluminum dissolution and sodium replacement with hydrogen, resulting in irreversible structural modifications. Changes in the silica-to-alumina ratio and sodium content were analyzed using a first-order Langmuir kinetic model at different temperatures, whereas enthalpy, entropy, activation energy, and frequency factor of adsorption were determined using the Van't Hoff and Arrhenius equations, with the first two having activation energies of 43,661.8 and 35,774.3 J/mol, respectively. The surface area and pore volume increased to 446.56 m^3/g and 446.56 cm^3/g, respectively, after 3 h at 75°C. XRD revealed minor distortions at the highest temperature and during extended treatment, resulting in slight alterations to particle size and crystallinity, highlighting the importance of optimizing acid treatment parameters to enhance zeolite properties while preserving structural integrity.

Keywords-acid treatment; Si/Al ratio; 13X zeolite; sodium removal; kinetics

I. INTRODUCTION

All standard zeolites are aluminosilicate minerals with a three-dimensional, microporous crystalline structure. They feature a unique combination of physical and chemical properties that make them useful in various industrial applications, agriculture, medicine, and environmental remediation [1]. Zeolites are widely used in chemical reactions, such as petroleum catalytic cracking, oligomerization, and fine chemistry, because of their activity and shape selectivity [2]. Zeolite activity is usually determined by the positions of Brønsted acid sites and metal phases that precipitate onto their structure [3]. The Brønsted acid sites are formed around aluminum atoms (Al) in H^+- form zeolites, which are

recognized as the source of zeolite catalytic activity [4]. A zeolite's catalytic and acidic properties are significantly influenced by its silica (Si) content and the Si/Al ratio. Additionally, improving the active sites within zeolite frameworks and modifying the acidity of siliceous or aluminous members of the substitutional series is possible through dealumination (for aluminous members) or desilication (for siliceous members) [5]. Efficient industrial applications require optimizing the Si/Al ratio because the amount of aluminum (Al) in the zeolite framework influences its properties, such as hydrophobicity and acidity. These properties affect catalytic behavior and hydrothermal endurance [6, 7]. Additionally, zeolites with low Si/Al ratios are susceptible to degradation through the elimination of Al species from the framework [8]. However, their application may not always be conducive to high Si/Al ratios, as in the selective catalytic reduction of NOx with NH_3. While a higher Si/Al ratio generally improves hydrothermal stability, it decreases the number of ion-exchange sites, including paired Al atoms that serve as sites for exchanging divalent cations, such as Cu^{2+} or Fe^{2+} [9]. Na-X zeolites, which are synthetic zeolites, have been investigated and employed in industrial chemical processes as ion exchangers, sorbents, and catalysts [10, 11]. Zeolites are widely used due to their ion exchangeability, shape selectivity, solid acid sites, and sizable void volume, comprising approximately 50% of the framework structure [12]. Na-X zeolites have a Faujasite (FAU) framework structure composed of a cage of $Na_{86}[AlO_{286}SiO_{106}]$. In (FAU)-type zeolites, 12-membered ring pore openings and the three-dimensional channel system arise from SiO_4 and AlO_4 tetrahedra that are linked by bridging oxygen atoms. These form supercages that host extra-framework cations and water molecules [13]. Acid treatment of Na-X zeolite, by removing aluminum (Al) atoms from its crystal structure (dealumination), can improve its catalytic properties and stability [14]. Various methods can be used, including treatment with citric acid ($C_6H_8O_7$) and ammonium fluoride (NH_4F) [15], steam treatment [16], and silicon removal followed by dealumination [17]. These methods are widely utilized to increase the Si/Al ratio in different zeolites. Acid treatment is one of the most common methods, because it improves the Si/Al ratio, increases porosity, and enhances thermal and chemical stability, enhancing catalytic and selective properties in reactions such as catalytic cracking. However, excessive treatment may result in dissolution of structural alumina or the formation of amorphous silicon, which can affect the zeolite's overall performance [5, 18]. The acid treatment of zeolite involves three main steps: First, zeolite with a high Na^+ content is exposed to an acidic solution in an ion exchange process. During this step, H^+ ions replaced the Na^+ ions in a cation exchange reaction. This transformation to H-zeolite enhances reactivity toward acid attack [19]. Second, Al was leached in an acidic environment, dissolving the tetrahedrally coordinated aluminum (Al^{3+}) ions from the zeolite framework and breaking the Al-O-Si bonds. Finally, extra-framework Al species are formed. A number of the leached Al^{3+} ions do not fully dissolve in the solution, but instead precipitate within the zeolite structure, either in the pores or on the surface, acting as Lewis's acid sources, contributing to the zeolite's overall acidity and catalytic properties. Thus, selectively removing Al increases the Si/Al ratio, modifies acidity, and improves thermal stability and catalytic performance [14]. Compared to intense acid leaching, treatment with citric acid preserves crystallinity better and allows for more controlled aluminum removal, modifying zeolites for use in catalysis, adsorption, and separation processes [20-22]. The zeolite was successfully modified by treating it with 0.1 N citric acid at 75 °C for 3 h to increase surface acidity and pore accessibility [23]. This research examines the acidic treatment process for Na-X zeolites using citric acid, analyzing how operating conditions affect chemical, textural, and crystalline properties. The study aims to investigate the impact of temperature and acid treatment time on zeolite-type Na-X properties. The results of the experiments and statistical analyses revealed the influence of operating conditions on zeolite properties. These properties include the Si/Al ratio and sodium content. Their kinetics were examined to observe how they change under acid treatment conditions. The treated Na-X zeolite was analyzed for textural properties, such as surface area and pore volume, and for characteristics such as crystal size and crystallinity.

II. EXPERIMENTAL METHOD

A. Experimental Design

Batch experiments based on a 3^2 fractional factorial design were conducted to examine the influence of citric acid treatment on the following properties:

- Chemical properties: Si/Al ratio and Na content
- Textural properties: Brunauer–Emmett–Teller (BET) surface area and pore volume
- Crystal properties: crystal size and crystallinity.

Table I shows the nine experiments and the two studied variables (temperature and time) at three selected levels. After conducting the optimization batch experiments, a regression analysis was performed to determine the statistical parameters of the study with 90% confidence intervals. Regression analysis was employed to determine the relationship between the independent variables and the response, in order to identify the optimal experimental settings.

TABLE I. GENERAL FACTORIAL DESIGN FOR 2 FACTORS WITH 3 LEVELS

Run	**1**	**2**	**3**	**4**	**5**	**6**	**7**	**8**	**9**
Time (h)	1	1	1	2	2	2	3	3	3
Temp. (ºC)	25	50	75	25	50	75	25	50	75

B. Experimental Procedure

The Na-X zeolite was prepared using the same materials and procedure without any modifications [23], treating 10 g of the Na-X zeolite, with a 150 mL solution of 0.2 M citric acid. The effects of the reaction time of the acid treatment (1 h, 2 h, and 3 h) and the temperature of the acid treatment (25 °C, 50 °C, and 75 °C) were studied. The temperature of the acid treatment was measured with an ASTM 15F mercury-filled glass thermometer (-1 °C-82 °C). The final product was then extracted by vacuum filtration. It was washed three times with deionized water to remove the Al complexes formed and dried

in an electric oven at 85 °C overnight. Then, the solid catalyst was calcined at 550 °C for 3 h and left to cool in a desiccator filled with silica gel until it reached ambient temperature.

C. Characterization Methods

Various characterization methods were used to analyze the prepared and modified Na-X zeolite samples. X-ray fluorescence spectrometry was employed to measure the composition of the original and treated samples of Na-X zeolite. BET measurements were performed using a Q-surf series analyzer (Italy) at the Ministry of Oil's Oil Development and Research Center to determine the samples' surface area and pore volume. XRD analysis was conducted using a D2 PHASER/Bruker instrument (Germany) with CuKα radiation and a nickel filter (λ = 1.5406 Å) to examine the crystal pattern of the prepared and modified Na-X zeolite in the 2θ range of 3-60°. XRD analysis was conducted at the Research Center for Materials at the Ministry of Science and Technology in Iraq. Crystal size and crystallinity were calculated for all samples using the Scherrer equation [24]:

$$D = \frac{0.95\lambda}{\beta \cos(\theta)} \quad (1)$$

$$\text{Crystallinity, \%} = \frac{Area\ under\ the\ crystalline\ peaks}{Area\ under\ all\ peaks} \times 100 \quad (2)$$

where D is the crystallite size in Å, k is the dimensionless crystallite shape factor (0.95), λ is 1.54056 Å, and β is the diffraction line broadening measured at a half maximum intensity in radians.

III. RESULTS AND DISCUSSION

A. Regression and Statistical Analyses

A full factorial design was constructed and the main and interactive effects were analyzed. This analysis included the Si/Al ratio, BET surface area, pore volume, crystal size, and crystallinity. The design yielded nine experiments with all possible combinations of the two factors (time and temperature). The studied factors, along with the reported responses, were measured three times, and the average values are presented in Table II.

TABLE II. EXPERIMENTAL DATA AND MEASUREMENT RESULTS OF ACID TREATMENT

Run	Time (h)	Temp. (ºC)	Si/Al	Na (%)	BET, (m^2/g)	Pore vol. (cm^3/g)	Crystal size (Å)	Crystallinity (%)
1	1	25	1.75	7.92	440.09	0.2622	5.9441	85.06
2	1	50	1.91	7.32	441.68	0.2634	5.9415	82.72
3	1	75	2.13	6.05	442.75	0.2641	5.9402	81.85
4	2	25	1.81	7.61	442.85	0.2627	5.9419	83.6
5	2	50	2.21	6.53	443.72	0.2645	5.9395	81.71
6	2	75	3.38	4.48	444.07	0.2673	5.9367	78.35
7	3	25	1.97	7.35	444.25	0.2656	5.9355	80.33
8	3	50	3.38	5.79	445.37	0.2732	5.9287	77.21
9	3	75	4.83	3.31	446.56	0.2773	5.9244	75.69
Original Na-X zeolite			1.71	8.23	437.22	0.2616	5.9468	88.03

A polynomial equation was adopted to describe the studied response surfaces mathematically, assuming a combination effect of factors as:

$$Y = a_o + a_1(t) + a_2(T) + a_3(t \times T) + a_4(t^2) + a_5(T^2) \quad (3)$$

where T is the temperature in °C and t is the treatment time in hours. Statistical calculations and regression analysis were used to fit the response function with experimental data. After neglecting coefficients with P-values greater than 0.1, the Fitted Mathematical Expressions (FMEs) with the highest correlation coefficients (R^2) and lowest possible Root Mean Square Error (RMSE) were selected. These values were incorporated into the final regression equation, which included all the coefficients shown in Table III. The statistical analysis showed that temperature was the most influential factor in altering the chemical properties (Si/Al and Na content) of acid-treated Na-X zeolite, which is consistent with previous kinetic and structural studies on zeolite dealumination [25]. In comparison, time had the most significant effect on changes in the texture and crystallinity of the treated Na-X zeolite.

TABLE III. FMES' REGRESSION RESULTS FOR THE STUDIED CHEMICAL, TEXTURAL, AND CRYSTAL PROPERTIES

Parameter	Si/Al	Na content (%)	BET (m^2/g)	Pore vol. (cm^3/g)	Crystal size (Å)	Crystallinity (%)
a_o	2.010	7.2970	437.532	0.2710	5.9368	90.5580
a_1	-0.5080	0.2783	1.9430	-0.0117	0.0119	-2.7330
a_2	-0.0175	0.0514	0.0413	-0.0001	9×10^{-6}	-0.0873
a_3	0.0248	-0.0217	-	-	7.2×10^{-5}	-
a_4	-	-	-	0.0028	0.0036	-
a_5	-	-0.0007	-	10^{-5}	-	-
Most contributing factor	Temp.	Temp.	Time	Time	Time	Time

B. Integrated Interpretation and FMEs Validation

Table IV presents the statistical evaluation of the FMEs describing chemical, physical, and textural properties and showing a high degree of consistency between the experimental data and the proposed mathematical representations.

TABLE IV. FMES STATISTICAL ANALYSIS

FMES	R^2	RMSE	Overall p-value	Max Cook's distance
Si/Al	0.9799	0.1879	1.16×10^{-4}	0.366
Na content (%)	0.9983	0.0904	8.79×10^{-6}	2.247
BET (m^2/g)	0.9773	0.3351	1.16×10^{-5}	0.744
Pore vol. (cm^3/g)	0.9820	0.0010	9.58×10^{-4}	2.243
Crystal size (Å)	0.9909	0.00088	2.48×10^{-4}	1.973
Crystallinity (%)	0.9564	0.7470	8.30×10^{-4}	0.290

The FME with a Si/Al ratio exhibited strong overall significance (p = 1.16×10^{-4}) and had excellent explanatory power (R^2 = 0.9799), with a low prediction error (RMSE = 0.1879). The maximum Cook's distance value of 0.366 indicates stable coefficient estimates and no influential observations, which supports the reliability of its interaction-driven structure. The Na content FME showed the highest goodness-of-fit (R^2 = 0.9983, RMSE = 0.0904) and significance (p = 8.79×10^{-6}) among all responses; however, its Cook's distance (2.247) suggests sensitivity to at least one data point. This is consistent with the inclusion of a quadratic temperature term that amplifies curvature effects and increases leverage. The BET surface area FME maintained a robust fit (R^2 = 0.9773, RMSE = 0.3351) and a statistically significant

overall model ($p = 1.16\times10^{-5}$). Its Cook's distance (0.744) is within acceptable limits, confirming the statistical stability of the linear dependence on time and temperature. The pore volume FME displayed strong significance ($p = 9.58\times10^{-4}$) and high explanatory power ($R^2 = 0.9820$), though its elevated Cook's distance (2.243) reflects nonlinear term influence, as expected given the pore-structure metric sensitivity to experimental perturbations. Similarly, the crystal size FME revealed a high-fidelity fit ($R^2 = 0.9909$, RMSE = 0.00088, $p = 2.48\times10^{-4}$). However, Cook's distance (1.973) suggests that certain observations significantly impact the quadratic-interaction structure, which is a common occurrence in size-related crystallographic responses. Finally, the crystallinity FME demonstrated strong overall significance ($p = 8.30\times10^{-5}$), satisfactory agreement with the data ($R^2 = 0.9564$, RMSE = 0.7470), and a low Cook's distance (0.290). This confirms the absence of influential points and supports the adequacy of the linear formulation for this response. Taken together, the high R^2 values, low RMSE magnitudes, and strong, model-wide significance across all six FMEs demonstrate their suitability for describing the underlying chemical and structural transformations. At the same time, the observed Cook's distances indicate which models are most sensitive to data leverage, and thus require cautious interpretation of nonlinear terms.

C. Effect of Operating Conditions on the Chemical Properties

The responses of the chemical properties (Si/Al and Na content) to the variables of the acid treatment process were studied, and the contour plots are shown in Figures 1 and 2. Figures 1 and 2 were plotted based on the parameters obtained from the statistical analysis of the experimental results for Si/Al and Na content. Changes in the Si/Al ratio of acid-treated Na-X zeolite are essential for understanding compositional changes. Figure 1 shows that the Si/Al ratio gradually increases from its initial value (1.71) for the original Na-X zeolite with both temperature and acid treatment time, reaching its highest value (4.83) at the maximum values of the two variables (75 °C and 3 h). The increase in the Si/Al ratio is due to the selective dissolution of Al from the zeolite framework. Since acid attacks Al more than Si in the zeolite structure, acid treatment reduces Al content and preserves Si. This results in a high Si/Al ratio in the treated samples [26]. The Si/Al ratio increases with temperature because thermal energy promotes bond breaking within the zeolite's crystalline structure, allowing Al to more easily exit the structure. Additionally, long-term acid treatment can cause the zeolite to recrystallize, which leads to structural changes that contribute to further loss of Al and subsequently increases the Si/Al ratio [9, 27]. Figure 2 portrays the contour plot of the change in sodium (Na) content in the treated Na-X zeolite under acid treatment conditions. The Na content decreases with increasing temperature and time. The highest sodium content is obtained after a short treatment at a low temperature and is slightly lower than the pre-treatment content (8.23%). As the temperature and treatment time increase, the kinetic energy of the ions increases, enhancing the efficiency of ion exchange and leading to a gradual decrease in Na content. The lowest value (3.31%) is reached at the highest temperature and treatment time. The reduction in Na content in Na-X zeolite during acid treatment occurs due to the increased efficiency of replacing alkaline ions, such as sodium, potassium, and lithium, with hydrogen ions (H^+), which decreases the Na content in the crystal structure [9]. Additionally, zeolites undergo a rearrangement of their crystal structure during prolonged, high-temperature acid treatment. This allows Na to leave the active sites, leading to a significant decrease in its concentration. Furthermore, acid treatment may partially dissolve some components of Na-X zeolite, resulting in the gradual removal of sodium trapped within the material's structure [28].

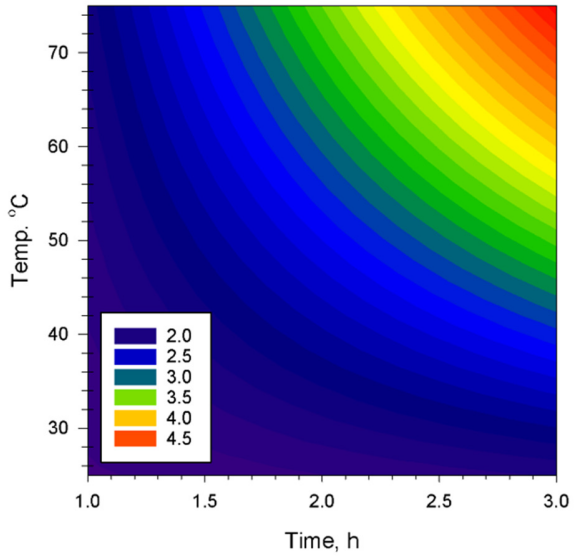

Fig. 1. Contour plot of the Si/Al ratio versus acid treatment temperature and time.

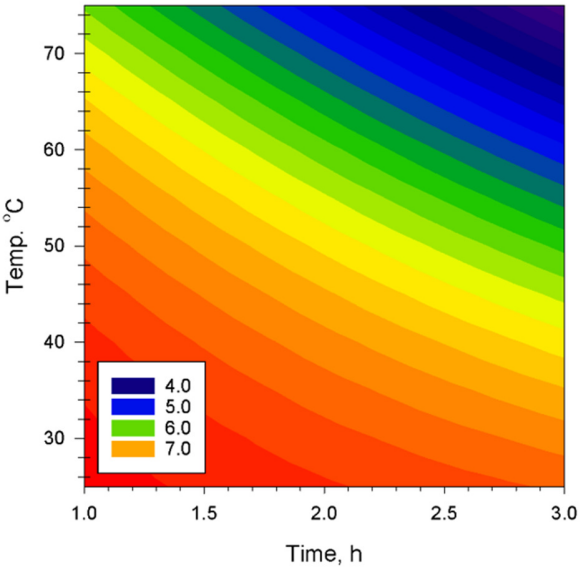

Fig. 2. Contour plot of the Na content versus acid treatment temperature and time.

Increasing the Si/Al ratio and decreasing the Na content after acid treatment effectively improves the quality of the

zeolites, enhancing their chemical and thermal stability and making them more suitable for various applications. Since both Al and Na stabilize the zeolites' crystalline framework, excessive acid treatment that depletes these elements may cause the crystal structure to collapse. Therefore, it is vital to monitor crystalline changes and ensure that the zeolite framework structure remains intact [29].

D. Kinetics of Si/Al Ratio and Na Content Change

The acid-treated zeolites undergo structural and chemical changes due to the selective dissolution of Al and the replacement of Na in the crystal lattice with H. This process is irreversible after dissolving [30]. Similarly, the Na^+ ions are replaced by the H^+ ions supplied by the acid during the reaction, which increases surface acidity—a difficult-to-reverse process. Therefore, the reactions that occur during acid treatment are irreversible because they lead to permanent changes. Without complex synthetic processes, such as hydrothermal crystallization or directed alkali addition, the original zeolite structure cannot be restored. Due to the abundance of H^+ and the irreversibility of the reaction, a first-order Langmuir kinetic model was adopted to describe the kinetics of increasing the Si/Al ratio and removing Na content [25, 31]:

$$Al - Zeolite_{(surface)} + H^+{}_{(aq)} \rightarrow Al^{3+} + H - Zeolite_{(surface)} \quad (4)$$

$$Na - Zeolite_{(surface)} + H^+{}_{(aq)} \rightarrow Na^+ + H - Zeolite_{(surface)} \quad (5)$$

$$-r_A = \frac{k_s C_A}{1+K_e C_A} = -\frac{dC_A}{dt} \quad (6)$$

where $-r_A$ is the reaction rate, C_A is the Si/Al ratio or Na content, k_s is the surface reaction rate coefficient, and K_e is the adsorption equilibrium constant. The K_e changes with temperature according to the Van't Hoff equation [32], and the k_s varies with the temperature according to the Arrhenius equation [33]:

$$K_e = exp\left(\frac{-\Delta H_{ads}}{RT}\right) exp\left(\frac{-\Delta S_{ads}}{R}\right) \quad (7)$$

$$k_s = k_o \, exp\left(\frac{-E}{RT}\right) \quad (8)$$

where ΔH_{ads} and ΔS_{ads} are the enthalpy and entropy changes of the adsorption step in J/mol and J/mol.K, respectively, R is the gas universal constant (8.314 J/mol.K), k_o is the reaction frequency factor in h^{-1}, E is the reaction's activation energy in J/mol, and T is the reaction temperature in K. The initial Si/Al ratio or Na content (C_{Ao}) was known, so combining (6) yields:

$$ln\left(\frac{C_{Ao}}{C_A}\right) + K_e(C_{Ao} - C_A) = k_s t \quad (9)$$

where K_e and k_s were found by the least squares technique using the experimental measurements of the change in the Si/Al ratio and Na content in Na-X zeolite with time (t) for each temperature (T) by building a program written in Python [34]. The obtained K_e and k_s values for the changes in the Si/Al ratio and Na content are presented in Table V for each acid treatment temperature. The K_e values are similar in magnitude at each temperature and increase with treatment temperature for both the Si/Al ratio enhancement and Na content reduction reactions. These results are consistent with the adsorption process, specifically chemical adsorption. Increasing the temperature improves adsorption efficiency by increasing diffusivity, which allows H^+ to reach the target sites on the zeolite surface more easily. As expected, the values of the reaction constants rise with the reaction temperature due to the increase in the kinetic energy of the reacting molecules, thus improving the number of effective collisions necessary to complete the reaction [34].

TABLE V. K_E AND K_S FOR Si/Al AND Na CONTENT CHANGE VERSUS THE TEMPERATURE OF ACID TREATMENT

Temperature (°C)	Si/Al		Na content (%)	
	K_e	k_s, (h^{-1})	K_e, 1/Na content	k_s, (h^{-1})
25	0.00124	0.02632	0.00128	0.03791
50	0.00138	0.17420	0.00139	0.11553
75	0.00139	0.32202	0.00141	0.30191

The results obtained for the adsorption equilibrium constants and reaction coefficients versus temperature were utilized to estimate the enthalpy and entropy of the adsorption step using the van't Hoff (7), as well as the reaction activation energies and frequency factors using the Arrhenius (8). Figure 3 displays the linear form of the Van't Hoff equation, which was obtained by plotting the log Ke against $1/T$. A straight line is formed with a slope of $-\Delta H_{ads}/R$ and an intersection point of $-\Delta S_{ads}/R$. The estimated values of ΔH_{ads} and ΔS_{ads} for both reactions are presented in Table VI. The ΔH_{ads} and ΔS_{ads} values indicate that dealumination requires more energy input than Na removal. The higher ΔH_{ads} for Si/Al indicates that Al removal from the zeolite framework is more energy-intensive than Na removal [25]. The ΔS_{ads} values were relatively close, indicating a similar degree of disorder introduced into the system during Si/Al ratio improvement and Na content removal. This agrees well with previously reported experiments on HY zeolite [35]. Similarly, Figure 4 presents the linear form of the Arrhenius equation, obtained by plotting $\ln(k_s)$ versus $1/T$, with a slope of $-E/R$ and an intercept of $\ln(k_o)$.

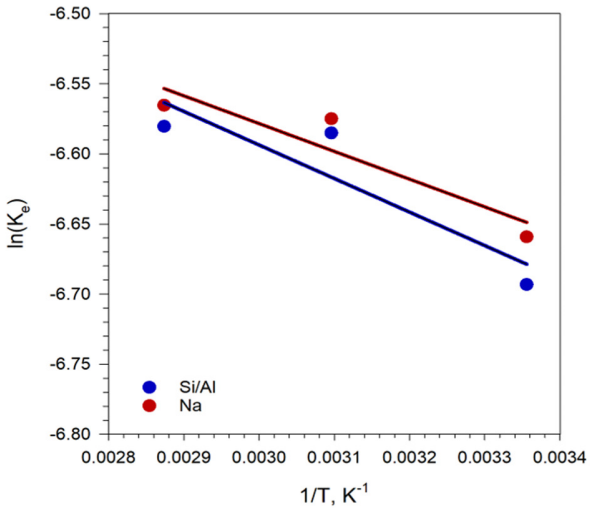

Fig. 3. Van't Hoff plot of the adsorption equilibrium constants of the Si/Na ratio and Na content change.

Table VII illustrates the E and k_o values for the two reactions, the improvement in the Si/Na ratio, and the removal of Na. The E values were 43,661.8 J/mol for the Si/Na ratio reaction and 35,774.3 J/mol for Na content removal. The k-value for the Si/Na-ratio-enhancing reaction was higher than that for Na-content removal (1.40×10^{6} versus 7.07×10^{4} h^{-1}). The higher activation energy of the Si/Al ratio-enhancing reaction compared to Na content removal indicates that Na content removal is less sensitive to temperature than the Si/Al ratio.

TABLE VI. ΔHADS AND ΔSADS FOR THE ADSORPTION OBTAINED BY THE VAN'T HOFF EQUATION

	ΔH_{ads} (J/mol)	ΔS_{ads}, (J/mol. K)	R^2
Si/Al	1987.38	48.8	0.8167
Na	1646.09	49.75	0.8583

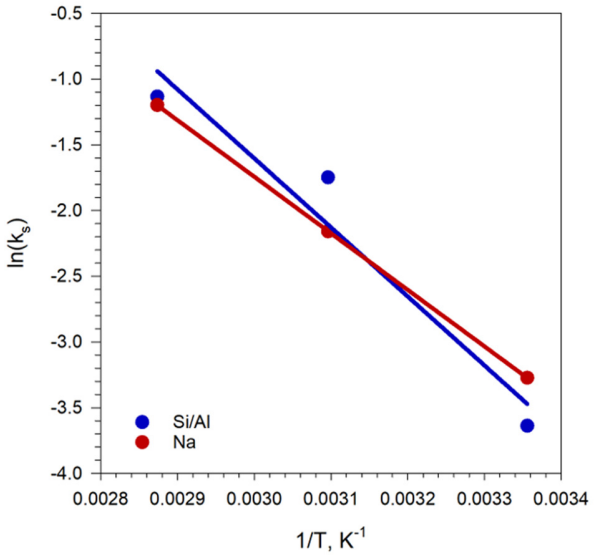

Fig. 4. Arrhenius plot for the Si/Na ratio and Na content change.

TABLE VII. ACTIVATION ENERGY AND FREQUENCY FACTOR FOR THE Si/Al RATIO AND Na CONTENT CHANGE

	E (J/mol)	k_o (h^{-1})	R^2
Si/Al	43661.8	$1.40\times10^{+6}$	0.9429
Na	35774.3	$7.07\times10^{+4}$	0.9991

E. Effect of Operating Conditions on the Textural Properties

The effect of citric acid treatment process variables on the textural properties of Na-X zeolite, including its BET surface area and pore volume, was examined using previously obtained parameters. Contour plots of the textural responses are shown in Figures 5 and 6 for surface area and pore volume, respectively. The BET surface area of Na-X zeolite increases from its original value of 437.22 m²/g with an increase in both treatment temperature and time. Similarly, the treatment temperature and time positively affected the pore volume of the treated Na-X zeolite. The improvement in BET surface area and pore volume indicates that operating conditions positively affect the porous structure of zeolite. At short processing times and low temperatures, a noticeable change in surface area and pore volume was observed (440.09 m²/g and 0.2622 cm³/g), as the conditions were insufficient for removing Al and Na from the Na-X zeolite framework. Increasing the treatment temperature and time to 75 °C for 3 h led to the significant removal of Al and Na from the zeolite crystal structure. This resulted in the opening of additional pores and an increase in the BET surface area and pore volume, reaching values of 446.56 m²/g and 0.2773 cm³/g, respectively. These surface area and pore volume results are consistent with known zeolite structural transformations under moderate acid treatment. Additionally, prolonged thermal treatment enhances void formation within the structure, which supports the increase in surface area and pore volume [36]. However, excessive acid treatment using high concentrations of acid, high temperatures, and long treatment times can lead to the partial or complete collapse of the zeolite crystal structure due to the dissolution of Al and release of Na, resulting in significant loss of surface area [23].

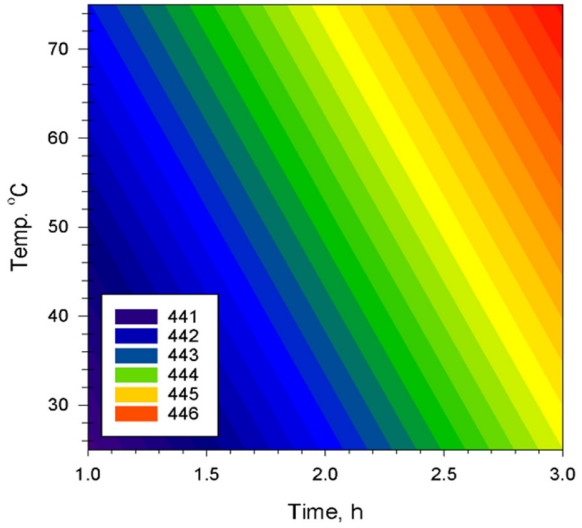

Fig. 5. Contour plot of the BET surface area versus acid treatment temperature and time.

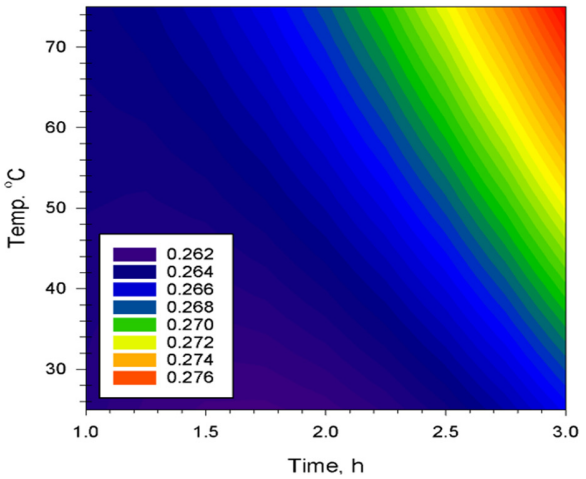

Fig. 6. Contour plot of the pore volume versus acid treatment temperature and time.

F. Effect of Operating Conditions on the Crystal Properties

XRD was used to evaluate the uniformity of the crystalline structure and confirm that the diffraction patterns of the treated Na-X zeolite samples remained intact. XRD examinations were performed on the original zeolite and the treated zeolite to confirm that the treatment conditions did not alter the diffraction pattern. Figure 7 depicts the XRD results for the original sample and for samples treated at the highest temperature for different lengths of time. The treated zeolite samples retained the main diffraction patterns of the original (untreated) Na-X zeolite, indicating that the treatment process did not significantly alter the crystalline structure of the samples under the current conditions. However, slight changes in peak intensity were observed with increasing temperature and treatment time. Figure 7 demonstrates a decrease in peak intensity and a slight increase in dispersion with treatment time from 1 h to 3 h at 75°C. This indicates a structural modification of the treated zeolite due to the replacement of components of the zeolite crystal lattice, specifically aluminum and sodium, with H^+. The XRD patterns of the original and treated Na-X zeolite agreed well with the standard Na-X zeolite (JCPDS card number 38-0237). These changes may worsen with prolonged treatment, leading to severe structural distortions in the treated zeolite, or even collapse of its crystal structure, with a significant portion transforming into irregular phases. These results highlight the importance of precise control over processing conditions, including temperature and time, to preserve the structural and crystalline properties of treated zeolite.

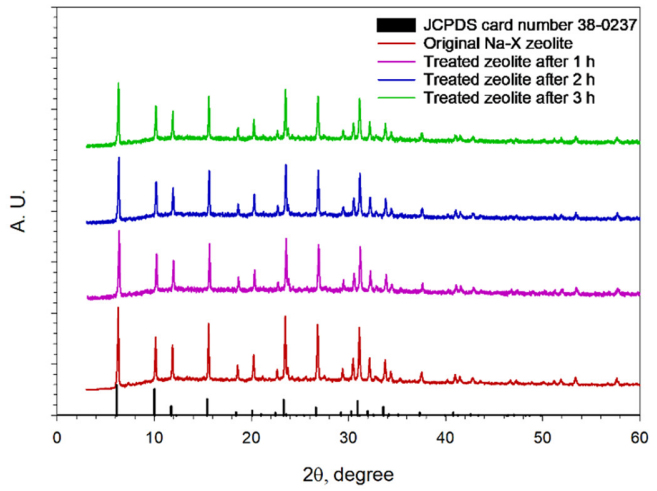

Fig. 7. XRD of the original and treated Na-X zeolite with 0.2 M CA at 75°C after different treatment times.

Figures 8 and 9 present contour plots of the crystal size and crystallinity of the treated Na-X zeolite as a function of the acid treatment temperature and time, respectively. The crystal size of the treated Na-X zeolite changed slightly from 5.9287 Å to 5.9468 Å. This indicates that the fundamental crystalline framework was partially damaged during the acid treatment process. However, XRD analysis revealed a slight decrease in crystallinity, from 88.03% for the original Na-X zeolite to 75.69%. Figure 9 shows that the reduction in crystallinity was more evident at higher temperatures and treatment times. This indicates that aggressive acid treatment conditions can disturb the long-range order of the material. This loss of crystallinity implies partial amorphization or structural rearrangement within the zeolite framework [37].

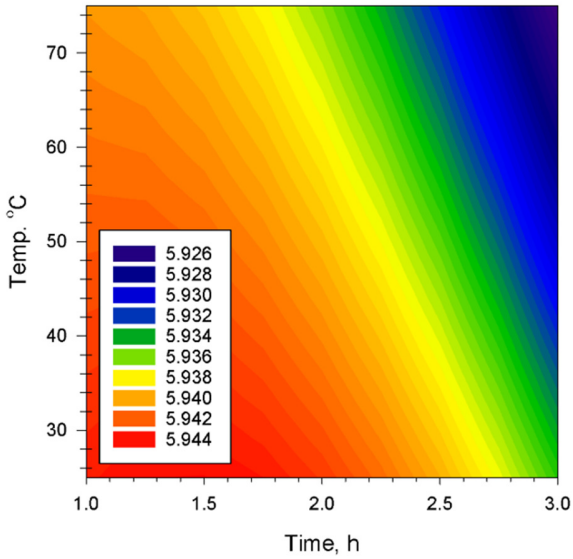

Fig. 8. Contour plot of the crystal size versus acid treatment temperature and time.

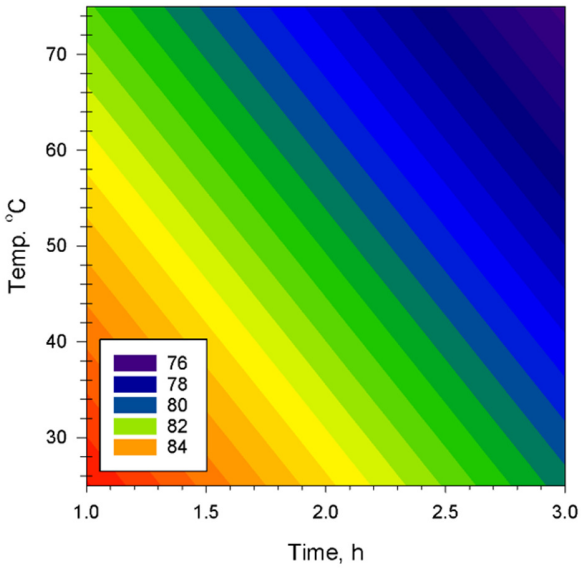

Fig. 9. Contour plot of the crystallinity versus acid treatment temperature and time.

IV. CONCLUSIONS

This study provided a comprehensive analysis of acid treatment by examining how operating conditions affect the chemical, textural, and crystalline properties of treated zeolite. A standardized analytical methodology was used for this analysis. The results offered valuable insights that contribute

significantly to current zeolite research and allow for a more consistent interpretation than previous studies. A factorial design approach was effectively applied to study the effects of alumina removal conditions on the properties of Na-X zeolite. Using citric acid in the treatment resulted in irreversible structural and chemical modifications to the zeolite, mainly due to the selective decomposition of aluminum and the replacement of sodium with hydrogen. The proposed conditions (75 °C for 3 h) increased the zeolite's surface area while maintaining its structural integrity. The data indicate that removing Al and Na significantly alters the material's chemical composition and structural properties. However, higher temperatures or longer treatment times decreased crystallinity, which could affect the modified Na-X zeolite's catalytic or adsorption performance. Kinetic analysis revealed that Al and Na removal were both temperature-dependent processes that followed a first-order Langmuir kinetic model. The adsorption equilibrium constants and reaction rate coefficients increased with temperature. The increase in K_e and K_s with temperature confirms that higher temperatures enhance the efficiency of removing the chemical components. The results showed that the activation energy for aluminum (Al) removal was higher than that for sodium (Na) reduction. Specifically, the activation energy for Al removal was 43,661.8 J/mol, while the activation energy for Na reduction was 35,774.3 J/mol. Textural and structural analyses revealed that controlled acid treatment increased the zeolite's BET surface area and pore volume, achieving the highest values at 75 °C with 3 h of treatment. However, prolonged or excessive acid treatment decreased crystallinity, resulting in partial amorphization and structural distortions. X-Ray Diffraction (XRD) analysis showed that the basic framework of the Na-X zeolite remained intact under mild treatment conditions. However, prolonged exposure resulted in slight decreases in peak intensity and increased dispersion. These results highlight the optimal operating conditions for acid treatment, balancing improvements in zeolite properties with structural integrity. Proper control of temperature and curing time is crucial for maximizing the benefits of acid modification and results in successfully modified zeolite without compromising its crystal stability.

REFERENCES

[1] G. W. Hardi, M. A. J. Maras, Y. R. Riva, and S. F. Rahman, "A Review of Natural Zeolites and Their Applications: Environmental and Industrial Perspectives," *International Journal of Applied Engineering Research*, vol. 15, no. 7, pp. 730–734, 2020.

[2] S. van Donk, A. H. Janssen, J. H. Bitter, and K. P. de Jong, "Generation, characterization, and impact of mesopores in zeolite catalysts," *Catalysis Reviews - Science and Engineering*, vol. 45, no. 2, pp. 297–319, 2003, https://doi.org/10.1081/CR-120023908.

[3] B. Xu, S. Bordiga, R. Prins, and J. A. van Bokhoven, "Effect of framework Si/Al ratio and extra-framework aluminum on the catalytic activity of Y zeolite," *Applied Catalysis A: General*, vol. 333, no. 2, pp. 245–253, Dec. 2007, https://doi.org/10.1016/j.apcata.2007.09.018.

[4] M. A. Deimund et al., "Effect of heteroatom concentration in SSZ-13 on the methanol-to-olefins reaction," *ACS Catalysis*, vol. 6, no. 2, pp. 542–550, Feb. 2016, https://doi.org/10.1021/acscatal.5b01450.

[5] A. Al-Nayili, M. Albdiry, and N. Salman, "Dealumination of zeolite frameworks and Lewis acid catalyst activation for transfer hydrogenation," *Arabian Journal for Science and Engineering*, vol. 46, no. 6, pp. 5709–5716, 2021, https://doi.org/10.1007/s13369-020-05312-w.

[6] E. A. Lombardo, G. A. Sill, and W. K. Hall, "The assay of acid sites on zeolites as measured by ammonia poisoning," *Journal of Catalysis*, vol. 119, no. 2, pp. 426–440, Oct. 1989, https://doi.org/10.1016/0021-9517(89)90172-3.

[7] R. Simancas et al., "Recent progress in the improvement of hydrothermal stability of zeolites," *Chemical Science*, vol. 12, no. 22, pp. 7677–7695, 2021, https://doi.org/10.1039/D1SC01179K.

[8] L. Shi et al., "The influence of adjacent Al atoms on the hydrothermal stability of H-SSZ-13: a first-principles study," *Physical Chemistry Chemical Physics*, vol. 22, no. 5, pp. 2930–2937, 2020, https://doi.org/10.1039/C9CP05141D.

[9] J. Li, M. Gao, W. Yan, and J. Yu, "Regulation of the Si/Al ratios and Al distributions of zeolites and their impact on properties," *Chemical Science*, vol. 14, no. 8, pp. 1935–1959, 2023, https://doi.org/10.1039/D2SC06010H.

[10] A. S. Zola, M. A. S. D. Barros, E. F. Sousa-Aguiar, and P. A. Arroyo, "Determination of the maximum retention of cobalt by ion exchange in H-zeolites," *Brazilian Journal of Chemical Engineering*, vol. 29, no. 2, pp. 385–392, Jun. 2012, https://doi.org/10.1590/S0104-66322012000200018.

[11] L. Singh, P. Rekha, and S. Chand, "Cu-impregnated zeolite Y as highly active and stable heterogeneous Fenton-like catalyst for degradation of Congo red dye," *Separation and Purification Technology*, vol. 170, pp. 321–336, 2016, https://doi.org/10.1016/j.seppur.2016.06.059.

[12] A. Corma, "State of the art and future challenges of zeolites as catalysts," *Journal of Catalysis*, vol. 216, nos. 1–2, pp. 298–312, 2003, https://doi.org/10.1016/S0021-9517(02)00132-X.

[13] C. Baerlocher, L. B. McCusker, D. Olson, and W. M. Meier, *Atlas of zeolite framework types*, 6th ed. Amsterdam, The Netherlands: Elsevier, 2007.

[14] H. Karami, M. Kazemeini, S. Soltanali, and M. Rashidzadeh, "The effect of acid treatment and calcination on the modification of zeolite X in diesel fuel hydrodesulphurization," *The Canadian Journal of Chemical Engineering*, vol. 100, no. 11, pp. 3357–3366, Nov. 2022, https://doi.org/10.1002/cjce.24350.

[15] T. Yoshioka et al., "Dealumination of small-pore zeolites through pore-opening migration process with the aid of pore-filler stabilization," *Science Advances*, vol. 8, no. 25, Jun. 2022, https://doi.org/10.1126/sciadv.abo3093.

[16] Y. Fan, X. Bao, X. Lin, G. Shi, and H. Liu, "Acidity adjustment of HZSM-5 zeolites by dealumination and realumination with steaming and citric acid treatments," *The Journal of Physical Chemistry B*, vol. 110, no. 31, pp. 15411–15416, Aug. 2006, https://doi.org/10.1021/jp0607566.

[17] M.-C. Silaghi, C. Chizallet, and P. Raybaud, "Challenges on molecular aspects of dealumination and desilication of zeolites," *Microporous and Mesoporous Materials*, vol. 191, pp. 82–96, Jun. 2014, https://doi.org/10.1016/j.micromeso.2014.02.040.

[18] H. Najar, M. S. Zina, and A. Ghorbel, "Study of the effect of the acid dealumination on the physico-chemical properties of Y zeolite," *Reaction Kinetics, Mechanisms and Catalysis*, vol. 100, no. 2, pp. 385–398, Apr. 2010, https://doi.org/10.1007/s11144-010-0189-8.

[19] O. Bortnovsky, Z. Sobalík, and B. Wichterlová, "Exchange of Co(II) ions in H-BEA zeolites: identification of aluminum pairs in the zeolite framework," *Microporous and Mesoporous Materials*, vol. 46, nos. 2–3, pp. 265–275, Aug. 2001, https://doi.org/10.1016/S1387-1811(01)00307-9.

[20] S. S. Vieira et al., "Use of HZSM-5 modified with citric acid as acid heterogeneous catalyst for biodiesel production via esterification of oleic acid," *Microporous and Mesoporous Materials*, vol. 201, pp. 160–168, 2015, https://doi.org/10.1016/j.micromeso.2014.09.015.

[21] Y. Yu, L. Zheng, and J. Wang, "Adsorption behavior of toluene on modified 1X molecular sieves," *Journal of the Air and Waste Management Association*, vol. 62, no. 10, pp. 1227–1232, Oct. 2012, https://doi.org/10.1080/10962247.2012.702186.

[22] S. Krachuamram, K. C. Chanapattharapol, and N. Kamonsutthipaijit, "Synthesis and characterization of NaX-type zeolites prepared by different silica and alumina sources and their CO2 adsorption properties," *Microporous and Mesoporous Materials*, vol. 310, Jan.

2021, Art. no. 110632, https://doi.org/10.1016/j.micromeso.2020.110632.

[23] B. A. Alshahidy and A. S. Abbas, "Preparation and modification of 13X zeolite as a heterogeneous catalyst for esterification of oleic acid," *AIP Conference Proceedings*, vol. 2213, 2020, https://doi.org/10.1063/5.0000171.

[24] A. L. Patterson, "The Scherrer formula for X-ray particle size determination," *Physical Review*, vol. 56, no. 10, pp. 978–982, Nov. 1939, https://doi.org/10.1103/PhysRev.56.978.

[25] Q. L. Wang, G. Giannetto, M. Torrealba, G. Perot, C. Kappenstein, and M. Guisnet, "Dealumination of zeolites II. Kinetic study of the dealumination by hydrothermal treatment of a NH4NaY zeolite," *Journal of Catalysis*, vol. 130, no. 2, pp. 459–470, Aug. 1991, https://doi.org/10.1016/0021-9517(91)90128-Q.

[26] X. Wang, O. Ozdemir, M. A. Hampton, A. V. Nguyen, and D. D. Do, "The effect of zeolite treatment by acids on sodium adsorption ratio of coal seam gas water," *Water Research*, vol. 46, no. 16, pp. 5247–5254, 2012, https://doi.org/10.1016/j.watres.2012.07.006.

[27] L. Zhang et al., "The effect and mechanism of Si/Al ratio on microstructure of zeolite modified ceramsite derived from industrial wastes," *Microporous and Mesoporous Materials*, vol. 311, Feb. 2021, Art. no. 110667, https://doi.org/10.1016/j.micromeso.2020.110667.

[28] S. Side, S. E. Putri, D. E. Pratiwi, A. Rahma, and Abd. Rahman, "The effect of acid treatment on the characteristics of modernite zeolite," *Sainsmat: Jurnal Ilmiah Ilmu Pengetahuan Alam*, vol. 12, no. 2, 2023, Art. no. 114, https://doi.org/10.35580/sainsmat122511932023.

[29] L. Velichkina, Y. Barbashin, and A. Vosmerikov, "Effect of acid treatment on the properties of zeolite catalyst for straight-run gasoline upgrading," *Catalysis Research*, vol. 1, no. 4, 2021, https://doi.org/10.21926/cr.2104004.

[30] P. Intharapat, S. Tontisirin, and C. Phalakornkule, "Effects of acid concentrations and acid treatment time on structural and textural characteristics of mesoporous zeolite 13X," *Materials Today: Proceedings*, vol. 77, pp. 1029–1032, 2023, https://doi.org/10.1016/j.matpr.2022.11.258.

[31] S. K. Kamal and A. S. Abbas, "Langmuir-Hinshelwood-Hougen-Watson heterogeneous kinetics model for the description of Fe(II) ion exchange on Na-X zeolite," *Engineering, Technology & Applied Science Research*, vol. 12, no. 5, pp. 9265–9269, Oct. 2022, https://doi.org/10.48084/etasr.5161.

[32] I. A. Stepanov, "The heats of chemical reactions: the Van't-Hoff equation and calorimetry," *Zeitschrift für Physikalische Chemie*, vol. 219, no. 8, pp. 1089–1097, 2005, https://doi.org/10.1524/zpch.2005.219.8.1089.

[33] O. Levenspiel, "Chemical Reaction Engineering," in *Chemical and Energy Process Engineering*, vol. 38, Boca Raton, Fl, USA: CRC Press, 1999.

[34] G. van Rossum, *Python Tutorial*, CWI Report CS-R9526, Centrum Wiskunde & Informatica, Amsterdam, The Netherlands, May 1995.

[35] T. Kasmi-Belouzir, A. Soualah, K. Kouachi, S. Mignard, and I. Batonneau-Gener, "Effect of acid-treated HY zeolites in adsorption of mesosulfuron-methyl," *Journal of Environmental Health Science and Engineering*, vol. 19, no. 2, pp. 1435–1445, 2021, https://doi.org/10.1007/s40201-021-00698-7.

[36] R. López-Fonseca, B. de Rivas, J. I. Gutiérrez-Ortiz, and J. R. González-Velasco, "Characterisation of the textural properties of chemically dealuminated Y zeolites," in *Studies in Surface Science and Catalysis*, vol. 144, pp. 717–722, 2002, https://doi.org/10.1016/S0167-2991(02)80201-4.

[37] S. K. Kamal and A. S. Abbas, "Decrease in the organic content of refinery wastewater by photocatalytic Fenton oxidation using iron-doped zeolite: Catalyst preparation, characterization, and performance," *Chemical Engineering and Processing - Process Intensification*, Sep. 2023, Art. no. 109549, https://doi.org/10.1016/j.cep.2023.109549.